coordinates of date (D) are derived from the fixed coordinates (F) by

$$\begin{pmatrix} x \\ y \\ z \end{pmatrix}_D = R' \begin{pmatrix} x \\ y \\ z \end{pmatrix}_F \tag{34}$$

The partials depend only on the partials of R', so that Eqs. (18) and (20) give

$$\left.\begin{aligned} \frac{\partial \tau_g}{\partial X} &= \frac{1}{c}\left[-\cos\delta\cos\lambda\, z/a + \sin\delta\, x/a\right] \\ \frac{\partial \tau_g}{\partial Y} &= -\frac{1}{c}\left[-\cos\delta\sin\lambda\, z/a + \sin\delta\, y/a\right] \\ \frac{\partial \nu_F}{\partial X} &= -\left(\frac{z\,\omega_e\cos\delta}{a\,\Lambda}\right)\sin\lambda \\ \frac{\partial \nu_F}{\partial Y} &= -\left(\frac{z\,\omega_e\cos\delta}{a\,\Lambda}\right)\cos\lambda \end{aligned}\right\} \tag{35}$$

It is to be understood that the x, y, z which appear in Eqs. (35) are in the fixed system. Order-of-magnitude calculations give 3 ns/m and 5×10^{-4} Hz/m the same as for the partials with respect to x, y, z.

Comparing the above order-of-magnitude calculations in Table 11 with the quoted accuracies of 300 ns and 0.003 Hz for a single run shows that the variables x, y, X, and Y are sensitive at the 5-m level, while α, δ, $\delta\epsilon$, and θ are sensitive at the 0.3 arc sec level and UT1 at the 20-ms level. Processing a number of runs together should allow reduction of these numbers, but it must be cautioned that simulations of the separability of the effects have not been carried out. No useful information is available on the z component of the baseline. Virtually all of the useful information comes out of the fringe rate. The key to more accurate time delays are wide bandwidths, while more accurate fringe rates will come from improved frequency standards.

By restricting consideration to fringe rate data only, it can be seen that maximum sensitivity to the baseline (or station position) comes at zero declination. Source position, precession and nutation constants, and UT1 improve with increasing equatorial projection of the baseline, while polar motion effects are most detectable with large polar-axis components of the baseline. The source right ascension, UT1, and polar motion are most accurately determined for sources at 0-deg declination, while the source declination and the precession and nutation constants θ and $\delta\epsilon$ are best determined for sources in the polar regions. The separation of the effects will require baselines with a variety of declinations and longitudes and sources with a variety of right ascensions and declinations.

References

1. Cohen, M. H., et al., "Compact Radio Source in the Nucleus of M87," *Astrophys. J. Letters*, p L83, 1969.
2. Melbourne, W. G., et al., *Constants and Related Information for Astrodynamic Calculations*, Technical Report 32-1306, Jet Propulsion Laboratory, Pasadena, Calif., Nov. 5, 1968.

B. Communications Systems Research

1. Information Systems: Performance of the Binary-Coded Sequential Acquisition Ranging System of DSS 14, W. L. Martin

a. Introduction. During September 1969 the Binary-Coded Sequential Acquisition Ranging System, described in SPS 37-52, Vol. II, pp. 46–49, and SPS 37-57, Vol. II, pp. 72–81, was installed at DSS 14. Through January 1970, when the station's operation was suspended for installation of the tri-cone, 46 separate ranging acquisitions had been made with *Mariners VI* and *VII*. Throughout the intervening 4 mo, several tests were conducted to accurately assess the performance of the ranging system in a DSS environment. This article summarizes the results of the tests performed and forms some conclusions regarding the potential of the tracking network.

b. System delay. Range is determined by accurately measuring the elapsed time between the transmission of a signal and its return to the tracking station. Delays inherent in the ground equipment and in the spacecraft's transponder are indistinguishable from those due to distance and must be subtracted from the measured range to yield its true value. Obviously, transponder calibration must be completed prior to launch since this act precludes any further testing. Fortunately, this is not true of the ground equipment, which is readily accessible and therefore can be examined quite thoroughly.

A unique property of this ranging system results from its use of RF doppler to simulate code doppler (see MacDoran and Martin, *Section A-4*, this chapter). The presence of charged particles along the signal ray path causes the code and clock dopplers to be shifted in frequency by nearly equal but opposite amounts. This results in a slow drift in the apparent range, which in

turn can be used to calibrate the charged-particle activity. Since a charged-particle calibration may require several hours, during which time the apparent range may change by only a few nanoseconds, it is important to know how much of this variation might be contributed by the equipment.

c. Ranging system delay stability. Prior to shipping the ranging system to Goldstone, a test was conducted to measure its internal delay and its delay stability. Figure 15 illustrates how the system was configured for this evaluation. A highly stable reference was supplied to two frequency synthesizers, which in turn acted as references for the RF and digital subsystems. A portion of the 10-MHz signal was bi-phase modulated, using a double balanced mixer, to provide the requisite input to the RF subsystem. An attenuator, placed between the modulator and the RF unit, was used to set the input level to approximately −100 dBmW. This relatively strong signal was employed so that any dc drift or delay variation would be readily discernible. Thus, the system was connected to literally range itself, providing not only a measure of its internal delay but also of its delay stability. It is important to understand that only the RF and digital subsystems described in SPS 37-57, Vol. II, were under test at this time. The equipment was allowed to warm up for 6 h prior to the calibration which commenced at 3 p.m. and lasted for a period of just under 2 h. All measurements were made in a laboratory environment.

Results of the test are shown in Fig. 16. The average delay was found to be 4.876 ns for the 102 sample points collected with a standard deviation of 13.9 ps. Drift rate was obtained by using least-squares criteria to fit a third-degree polynomial to the data. When completed, the average drift over the test period was found to be only 9.6 ps/h. This corresponds to a drift in range of about 0.05 in./h.

One of the more obvious conclusions to be reached from this test is that delay stability of the ranging system will not be a limitation to accuracy in the foreseeable future. Moreover, it has been suggested that the system may have some value as a calibration tool for spacecraft ranging transponders. To be useful in this capacity, additional interfacing hardware would be required to translate the signal to the proper S-band frequency.

d. Ranging at DSS 14. Performance of the ranging equipment in a DSS environment, which includes the associated transmitting, receiving, and antenna equipment, is of greater concern to the experimenter. Important parameters include total system delay, long- and short-term delay stability, delay dependence upon signal level, and reacquisition integrity.

System delay. Prior to each ranging pass, the entire ground system is calibrated to determine its delay. The

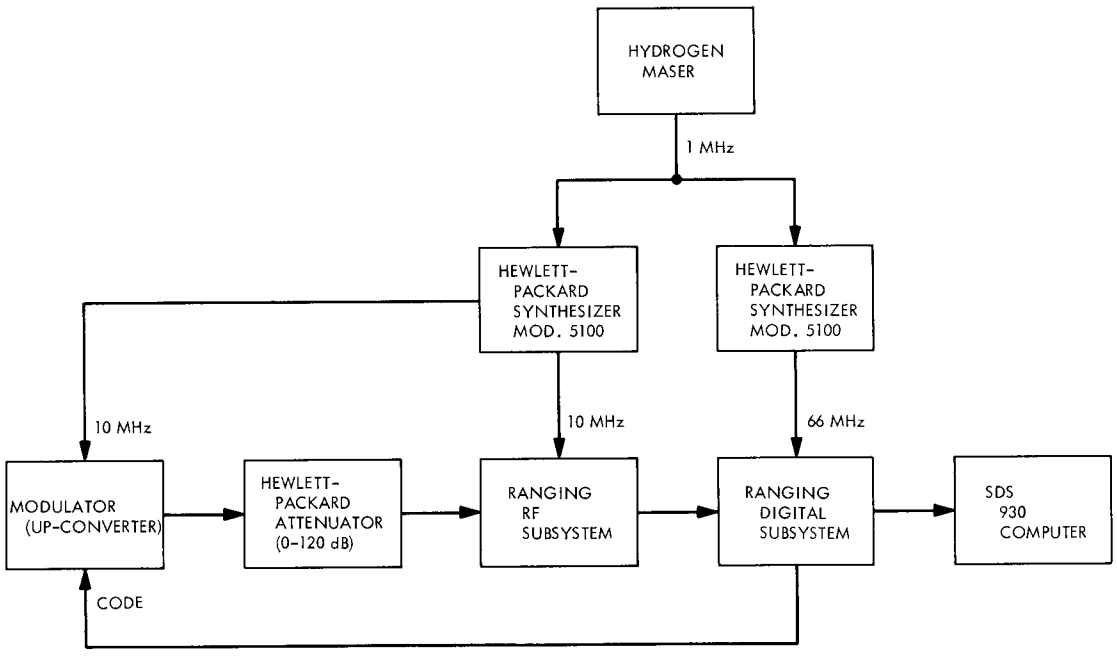

Fig. 15. Ranging system laboratory test configuration

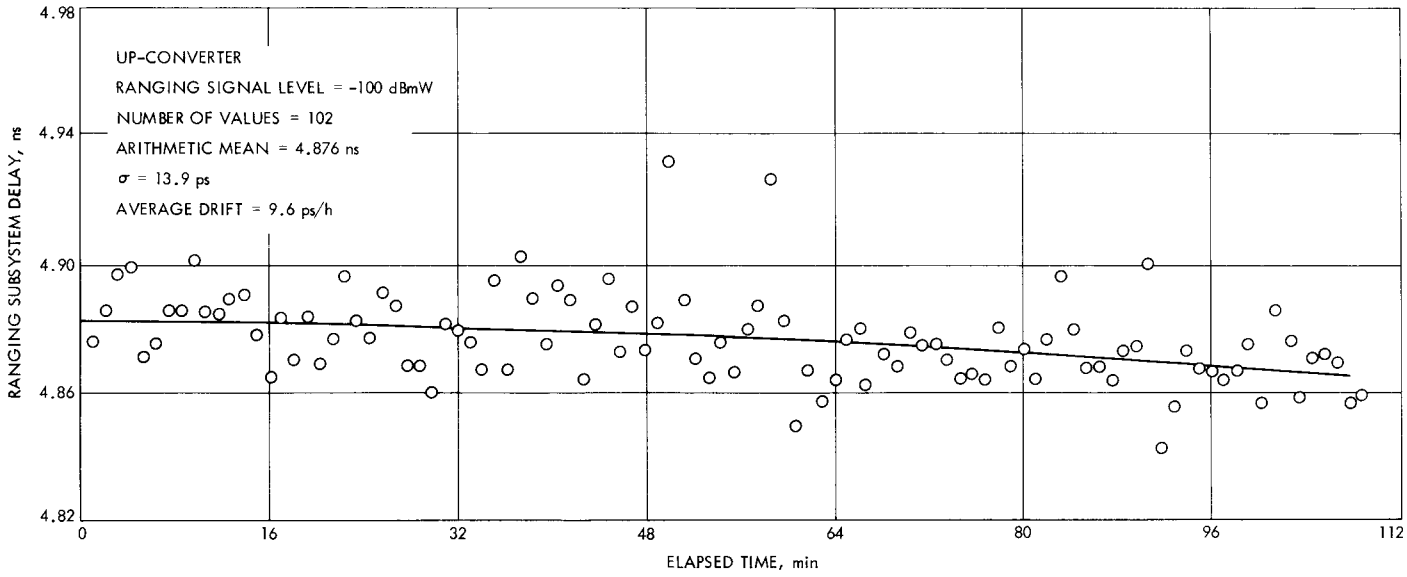

Fig. 16. Ranging subsystem drift (Jul 31, 1969)

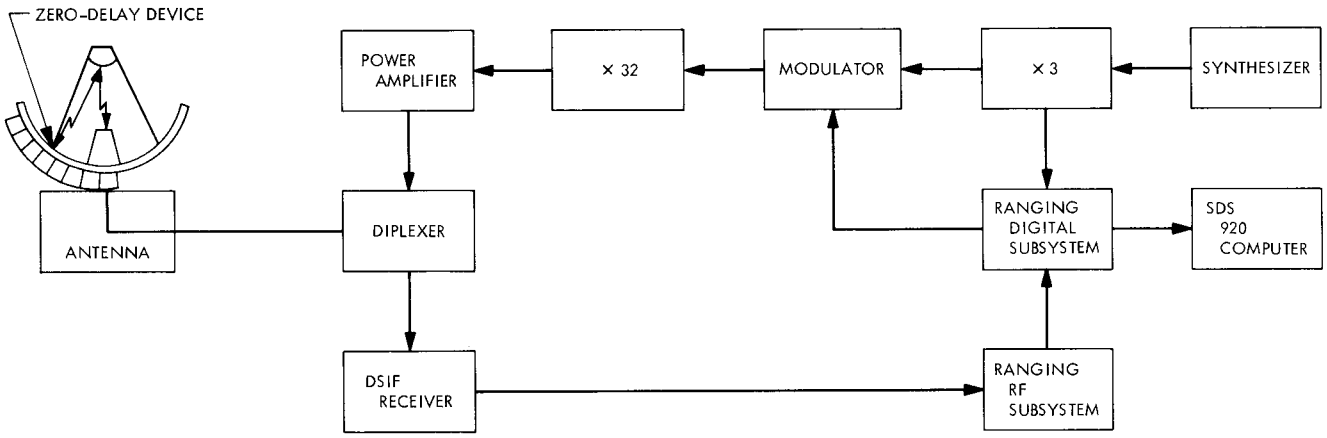

Fig. 17. DSS 14 ranging test configuration

system is configured with the antenna at zenith and the transmitter operating at full power, modulated by the ranging code (Fig. 17). A small crystal mixer (termed a zero-delay device) is located on the antenna surface near one of the quadrupods. Its purpose is to convert a portion of the transmitted signal to the receiver frequency $[\omega_R = (240/221)\omega_T]$ without introducing a significant delay. This translated frequency re-enters the horn and is processed by the DSIF receiver. The magnitude of the received signal is adjustable via an attenuator from above −100 dBmW to well below the receiver's threshold. Thus, it is possible to calibrate the delay of the ground equipment normally used with a spacecraft, and under virtually identical conditions. This delay, measured in microseconds, must be subtracted from the calculated range to yield its true value.

Long-term stability. Long-term delay stability can be assessed by comparing calibration numbers over several weeks. A 2-mo period from November 22, 1969 through January 24, 1970 was selected which included 12 data points (Fig. 18). The mean value for the total system delay throughout the period was found to be 3.34 μs (501 range meters) while the standard deviation was computed at 26 ns (3.9 range meters). A least-squares linear fit to the data shows a slope of −15 ns/mo (−2.2 range meters per month).

Long-term stability is mainly of academic interest since variations can be removed by daily calibration. However, it does provide some information about the inherent stability of a typical DSN station. It demonstrates, for example, that the delay drift is less than 0.5% per

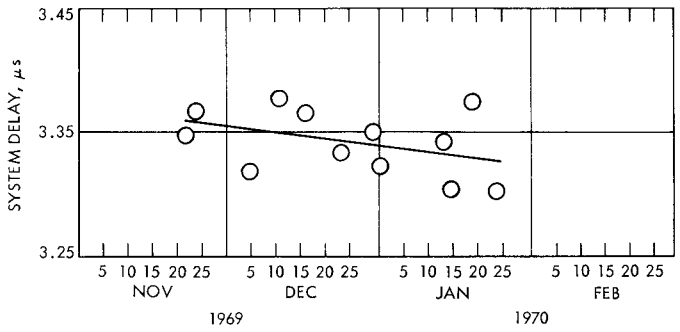

Fig. 18. Long term stability

month, which is a remarkable achievement for a system of that size and complexity. Moreover, the small value for σ suggests that one could forego range calibrations, using instead a standard value of 3.34 μs, and still be within the 5-m error budget.

Short-term stability. Short-term delay stability extending throughout a single pass is of more direct concern to the experimenter. As previously noted, during a charged-particle experiment, it is important to know how much of the range signature is attributable to system drift. Two investigations at different signal levels were conducted. The first on November 4, 1969 was made at −185 dBmW and covered an 8-h period (Fig. 19), while the second on December 6, 1969 at −170 dBmW had a duration of approximately 5 h (Fig. 20).

Results of the first test show an average delay of 3.26 μs over the 8-h period with a $\sigma = 20.2$ ns (Fig. 19). Observe that the average delay is somewhat less than that indicated on Fig. 18. The explanation is that the measurement was made shortly after the equipment was installed at Goldstone. Subsequent equipment and cabling modifications caused a slight increase in the total delay.

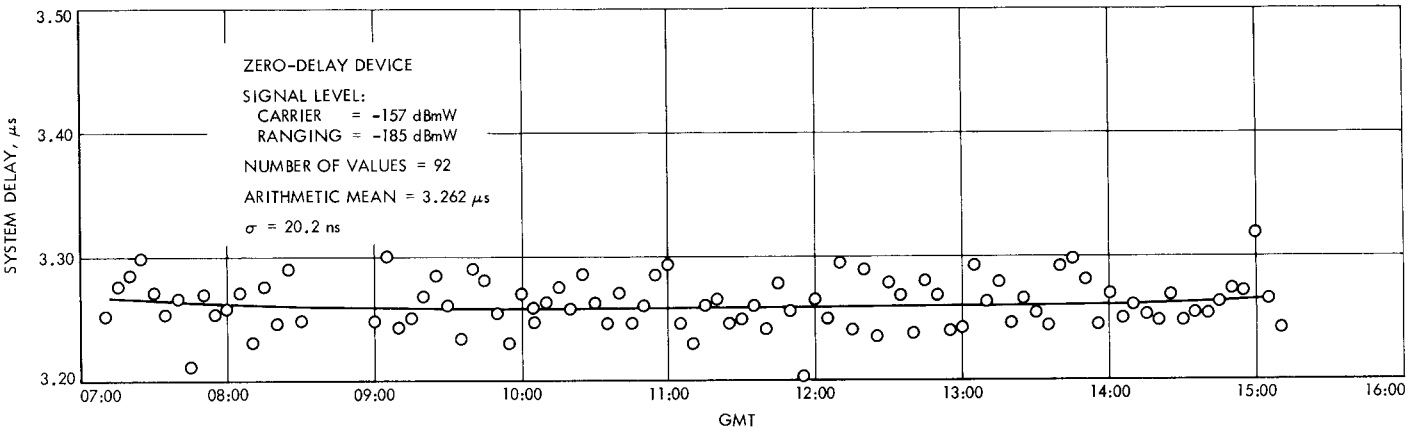

Fig. 19. Ranging system drift (Nov 4, 1969)

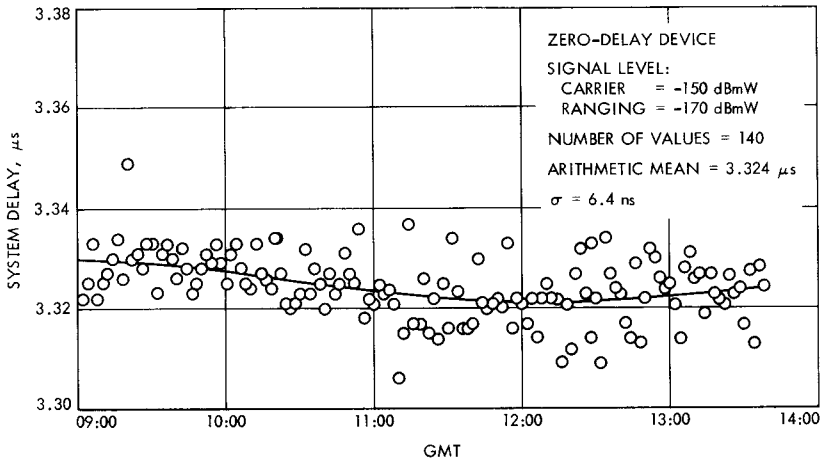

Fig. 20. Ranging system drift (Dec 6, 1969)

By using least-squares criteria to fit a third-degree polynomial through the data, the peak change was found to be 7.6 ns (1.1 range meters) over the 8-h period. This corresponds to an average change of 1.9 ns/h (0.285 range meter per hour) since the minimum appears to occur about midpass at 11:00 GMT. The maximum rate of change appears near the end of the test where it increases to 2.9 ns/h (0.43 range meter per hour).

This data is largely corroborated by the second test one month later when the average delay was found to be 3.324 μs. A decline in σ to 6.4 ns can be attributed to the relatively stronger signal and to a difference in the integration time. Fitting a third-degree polynomial to the data, the peak variation was measured at 9.2 ns (1.3 range meters) over the 3.5-h period. Average drift was computed to be 2.6 ns/h (0.39 range meter per hour) with a maximum slope of 3.7 ns/h (0.5 range meter per hour) occurring at 10:30 GMT.

Several remarks can be made regarding these investigations. Note that the minimum delay appears in both tests at approximately the same time (11:00–12:00 GMT). This suggests that the drift may have a diurnal character. An explanatory model is difficult to formulate since the reversal takes place between 3:00 and 4:00 a.m. PST. The obvious supposition of a thermal stimulus is awkward to justify since nearly 9 h have elapsed since there were any important thermal inputs. Variations in the plenum temperature are either too small to be measured or are not correlated with the observed excursions. Coaxial cables, the most likely point of thermal influence because of the quantity involved, can be discarded since measurements indicate a change of only 10 ps per degree of temperature rise per 100 ft. The maxima and minima in the delay, particularly evident in the December 6 run, together with almost identical excursions for the two tests, imply a limit cycle process of a massive system—massive because the time constant is clearly several hours. Power line variations, plausible from a timing consideration, become impractical as an explanation because of the excellent voltage regulation employed. Summarizing, additional testing over considerably longer time periods will be required to isolate the source of the drift.

In any event, the data indicates that the maximum drift to be experienced over a pass will be less than 1.5 m. Fortunately, a variation of this magnitude is within the error budget for *Mariner* Mars 1971. Similarly, maximum short-term drift rates of 0.5 m/h are believed to be adequate for charged-particle investigations provided that the limit of 1.5 m per pass is not exceeded.

Signal level dependency. System delay variations resulting from changes in the received signal level are another source of error. Phase shifts in the ground receiver's IF amplifiers vary slightly with automatic gain control voltage, causing the system delay to be dependent upon signal level. This problem is particularly acute in the spacecraft's transponder where changes as great as 1 m of range per dB of signal level have been observed.

An investigation was conducted on November 12, 1969 to ascertain the extent of the delay variation in the ground equipment. The system was configured as shown in Fig. 17 with the transmitter operating at 20 kW. Ranging and carrier power were set for −100 dBmW and an acquisition was initiated. After collecting a suitable number of range points, the power was reset to −130 dBmW without breaking lock. This procedure was repeated once more to reduce the level to −160 dBmW.

Results of the test appear in Fig. 21 and indicate that the change in system delay is less than 1 ns (0.15 range meter) over the 60-dB range. Some uncertainty arises in the last set of points due to the large value of σ. However, evidence obtained in a later test, in which reacquisition

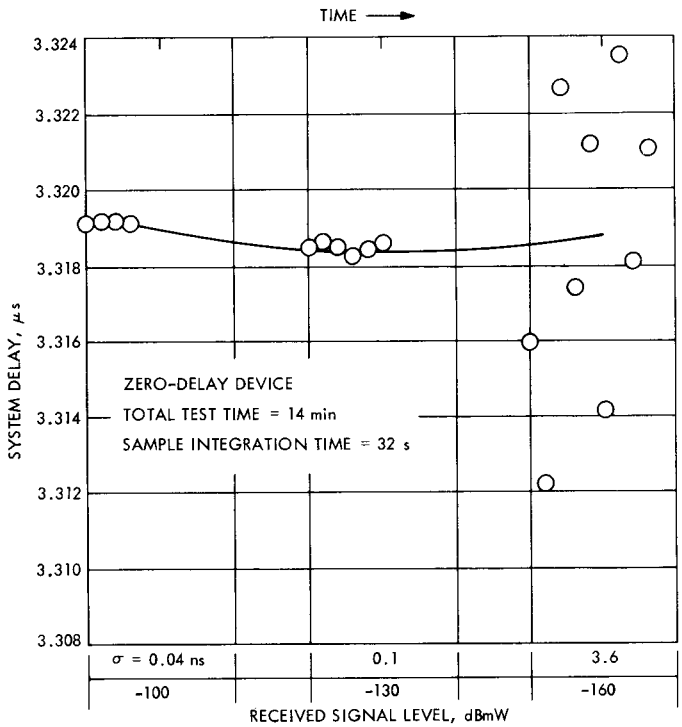

Fig. 21. Signal level stability

follows each signal level change, substantiates the independence of system delay and signal strength. The data of Fig. 21 also includes any drift that may have taken place during the 14-min test period but this should not exceed 1–2 ns.

It can be concluded from this experiment that the received signal level does not grossly influence the system delay, unlike the behavior of the spacecraft's transponder. When drift is accounted for, the delay should not change by more than 2 ns (0.3 range meter) over a 60-dB signal range. In most situations, even for long data arcs, the error due to signal strength fluctuations should be well below 1 ns (0.15 range meter).

Acquisition integrity. Consider a stationary target at a known distance. Each acquisition should produce an identical number representing the correct range. The extent to which this is true is a measure of the system's acquisition integrity. Reasons for poor integrity would be delay drift, insufficient resolving power, and poor noise performance.

An experiment was conducted on November 12, 1969 to measure the acquisition integrity of the ranging equipment. System configuration was identical to that employed in the previous signal level dependency test. Seven acquisitions were obtained, each at a different received signal strength. The first set of measurements was made at −100 dBmW. The signal level was then reduced by 10 dBmW and a reacquisition initiated. The purpose of this test was to explore the acquisition integrity and its dependence upon received signal power.

Results of the investigation are plotted in Fig. 22. A 3-ns variation was found to exist throughout the test period which lasted slightly less than 1 h. Careful examination of the points, particularly at strong signal levels, reveals a very definite trend. The points within a given set clearly describe an arc with very little scatter. Therefore, it is reasonable to assign the nonlinearity of the data to delay drift and not to the reacquisition process. Spaces that represent the reacquisition process have been left between the sets of points and an average curve has been fitted to the data.

Two conclusions to be reached from this investigation are:

(1) Reacquisition introduces no major discontinuities. Had the lock not been broken the data would continuously follow the average curve in Fig. 22.

(2) The data also confirms the previous finding that there are no significant variations in delay resulting from signal level changes.

The magnitude and period of the drift are of some concern. Quite possibly the drift is due to temperature variations within the cone located on the antenna structure. During this test an operator was present in the cone to adjust the signal level, and temperature fluctuations could have resulted from his opening and

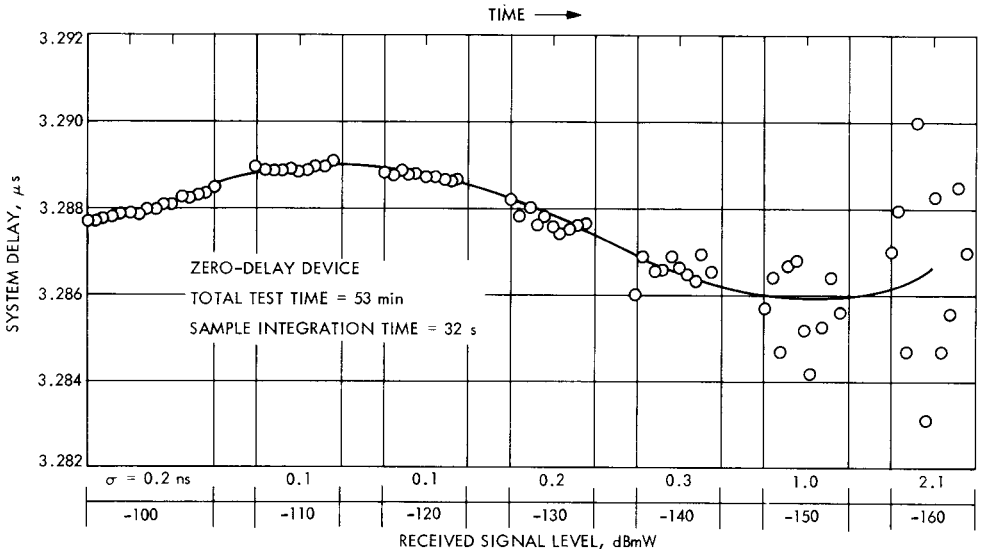

Fig. 22. Reacquisition and signal level test

closing the door and the equipment cabinets. Additional tests will be necessary to isolate the source.

e. Conclusions. These investigations have provided experimenters with the following information regarding the DSN ranging capability:

(1) The ranging system introduces no significant delay or delay drift.

(2) The long-term stability of DSS 14 is excellent since the delay changes by only 2.2 m (0.5%) per month.

(3) The short-term drift extending over one pass is less than 1.5 m although slopes as great as 0.5 m/h have been observed.

(4) No significant change in the delay of the ground equipment was found by varying the input signal over a 60-dB range.

(5) Reacquisition introduces no observable discontinuities in the ranging data.

Two additional tests are required for clarification of the system's performance. First, a closed-loop ranging calibration covering a continuous 24-h period should be obtained to determine whether the drift has a diurnal character. Second, the system should be calibrated at several different antenna angles to discover if the antenna's position influences the delay. This information, together with that previously obtained, should provide a complete understanding of DSN ranging.

2. Information Systems: Buffer Parameters and Output Computation in an Optimum Convolutional Decoder, *J. W. Layland*

a. Introduction. The impressive results obtained by Heller (SPS 37-54, Vol. III, pp. 171–177) for the decoding of short constraint length convolutional codes by the Viterbi algorithm have motivated work aimed at the design of special-purpose equipment to implement this type of decoding. Heller's results showed the need for a buffer of 3 to 5 constraint lengths (K) for each of the 2^{K-1} states of the convolutional encoder. Since this is the largest single identifiable item in the decoder, and may, in fact, be the limiting factor for decoding speed, a more precise knowledge of the behavior of this buffer is needed. This article reports the results of a series of simulations which were performed to obtain that knowledge. The initial part of this series was performed using modified versions of Heller's program; the remainder was performed using the faster decoding program described in the following article, *Subsection 3.*

b. Problem statement. A convolutional code of constraint length K and rate $1/V$ may be thought of as a finite state machine with one input bit and V output bits per cycle, and 2^{K-1} possible states. For each state of the encoder, the optimum convolutional decoder must remember the most-likely bit stream (the *survivor*) leading to that state, and the likelihood of that survivor. Theoretically, the length of the survivors is infinite, since there is no finite length at which all of them must converge (Ref. 1). However, convergence may be forced by the inclusion of K or more known bits periodically into the data, as was suggested in the original description of the algorithm (Ref. 2). As a practical matter, however, convergence is rapid enough so that truncation of the survivor memory at a few constraint lengths will introduce only slight degradation in performance. The degradation suffered is a function not only of the length of the survivors but also of the method by which the output data stream is constructed from the 2^{K-1} survivors.

c. Decoder output construction. In previous simulations of this decoding algorithm, the output bit at each step was selected to be the oldest bit associated with the most-likely state. Depending upon the organization of the decoder, the selection of the most-likely state may be almost trivial, or it may be a rather large portion of the decoder. In the latter case, other methods of constructing the output data stream may be preferable. Another reasonable choice for selection of the data output is the majority function of the oldest bits of each of the 2^{K-1} survivors. Intuitively, it would seem that in most cases, where not all of the survivors were identical at their trailing ends, more would agree with the correct bit than would disagree. This has been borne out by simulation. The third output method that appears reasonable is the selection of the oldest bit in some arbitrarily chosen survivor.

These three techniques are compared in Figs. 23a, b, and c for $K = 4$, 6, and 8. The arbitrary state was, in each case, the all 1's state, the complement of the correct data. The curves are shown for an error probability close to 5×10^{-3}, a design point typical of deep-space missions. Each curve represents 10^5 decoded bits. The design tradeoffs can be easily specified for these three output techniques: if the arbitrarily selected survivor is used as a standard, a majority function output is approximately equal in value to an additional one and one-half constraint lengths in every survivor, and selection of the most-